^{129}Xe NMR Spectroscopy Study of Porous Cyanometallates

E. Lima,[†,‡] J. Balmaseda,[†,§] and E. Reguera*[,§,||]

Universidad Autónoma Metropolitana-Iztapalapa (UAM-I), México, Universidad Nacional Autónoma de México (UNAM), Instituto Politécnico Nacional (México) (IPN), and Universidad de La Habana (UH), Cuba

Received December 15, 2006

Zinc and cadmium hexacyanocobaltates(III) were prepared, and their porous networks were explored using ^{129}Xe spectroscopy. The crystal structures of these two compounds are representative of porous hexacyanometallates, cubic (*Fm*-3*m*) for cadmium and rhombohedral (*R*-3*c*) for zinc. In the cubic structure, the porosity is related to systematic vacancies created from the elemental building block (i.e., the hexacyanometallate anion), whereas the rhombohedral (*R*-3*c*) structure is free of vacant sites but has tetrahedral coordination for the zinc atom, which leads to relatively large ellipsoidal pores communicated by elliptical windows. According to the Xe adsorption isotherms, these porous frameworks were found to be accessible to the Xe atom. The structure of the higher electric field gradient at the pore surface (*Fm*-3*m*) appears and is accompanied by a stronger guest−host interaction for the Xe atoms and a higher capacity for Xe sorption. For cadmium, the ^{129}Xe NMR signal is typical of isotropic movement for the Xe atom, indicating that it remains trapped within a spherical cavity. From spectra recorded for different amounts of adsorbed Xe, the cavity diameter was estimated. For the zinc complex, ^{129}Xe NMR spectra are asymmetric because of the Xe atom movement within an elongated cavity. The line-shape asymmetry changes when the Xe loading within the porous framework increases, which was ascribed to Xe−Xe interactions through the cavity windows. The Xe adsorption revealed additional structural information for the studied materials.

1. Introduction

Cyanometallates form a family of porous molecular materials with relatively large amounts of free space (pore volume) and small access windows. Such structural features are attractive for the separation and storage of small molecules. In this sense, porous hexacyanocobaltates have been used, for instance, in the study of molecular hydrogen storage in molecular porous materials.[1−3] Some nitroprussides (pentacyanonitrosylferrates), for instance, are the most efficient H_2 storage materials on the basis of porous coordination compounds reported to date.[4] However, the porous framework properties of cyanometallates remain poorly documented, even when these compounds show a high flexibility to modulate the geometry, size, and physical features of the pore system. This communication represents a contribution in that sense. The porous nature of the cyanometallate structure is related to the coordination adopted by the metal (M) that forms the salt of the involved complex cyanometallate anion. In hexacyanometallates(III) of divalent transition metals, for instance, two types of porous frameworks are found. When the metal adopts an octahedral coordination, one-third of the anionic octahedral block sites remain vacant to form a network of large pores (ca. 8.5 Å) communicated by relatively small windows (ca. 4.2 Å) (interstitial free spaces).[5] However, when the metal is tetrahedrally coordinated to the N ends of the CN groups, a porous framework is also obtained but without vacant sites in the crystal structure.[6] In this case, the resulting pores have an ellipsoidal form (ca. 5.1 × 12.7 × 8.3 Å) and are communicated by elliptical windows (ca. 3.9 × 5.2 Å[7]). Cadmium and zinc hexacyanocobaltates(III) (cubic, *Fm*-3*m*) and rhombohedral (*R*-3*c*, based on a hexagonal cell) crystal structures, respectively, are representative of these two porous frameworks and also of porous hexacyanometallates (Prussian blue analogues). Anhydrous samples of these two compounds were studied from Xe adsorption isotherms and ^{129}Xe NMR spectra, and the obtained results are discussed in this contribution. Mixed Zn−K hexacyanoferrate(II) and its analogues of Na, Rb, NH_4, and Cs also crystallize in the *R*-3*c* rhombohedral cell,[8] but their pores were found to be inaccessible to Xe, even under pressure and at high temperature. Such behavior was attributed to the exchangeable cations that are situated close to the pore windows. Cadmium and zinc nitroprussides were initially included in this study, but their porous frameworks were also found to be inaccessible to the Xe atom. To the best of our knowledge, this is the first study using ^{129}Xe NMR spectroscopy on this family of porous materials.

2. Experimental Section

The studied samples were prepared using the precipitation method. Hot aqueous solutions (0.01 M at ∼90 °C) of zinc and cadmium sulfates and of $K_3[Co(CN)_6]$ were mixed under stirring, and the precipitate that was formed was aged 2 days within the mother liquor. The obtained solids were separated by centrifugation, washed several times with distilled water, and then air-dried at 60 °C. All the reagents used were analytical grade and were obtained from Sigma-Aldrich. The nature of the obtained powders as hexacyanometallates was verified from infrared (IR) spectra, and their stoichiometry was inferred from the atomic ratio of the involved metals, which was estimated from X-ray fluorescence analyses. The

* To whom correspondence should be addressed. E-mail: ereguera@yahoo.com.

† Instituto de Investigaciones en Materiales.

‡ Universidad Autónoma Metropolitana-Iztapalapa.

§ Instituto de Ciencia y Tecnología de Materiales.

|| Centro de Investigación en Ciencia Aplicada y Tecnología Avanzada.

(1) Kaye, S. S.; Long, J. R. *J. Am. Chem. Soc.* **2005**, *127*, 6506.

(2) Chapman K. W.; Southon P. D.; Weeks C. L.; Kepert C. J. *Chem. Commun.* **2005**, 3322.

(3) Hartman, M. R.; Peterson, V. K.; Liu, Y.; Kaye, S. S.; Long, J. R. *Mater. Chem.* **2006**, *18*, 3221.

(4) Culp, J. P.; Matranga, C.; Smith, M.; Bittner, E. W.; Bockarth, B. *J. Phys. Chem. B* **2006**, *110*, 8325.

(5) Ludi, A.; Gudel, H. U. *Struct. Bonding* **1973**, *14*, 1.

(6) Balmaseda, J.; Reguera, E.; Rodriguez-Hernandez, J.; Reguera, L.; Autie, M. *Microporous Mesoporous Mater.* **2006**, *96*, 222.

(7) Cartraud, P.; Cointot, A.; Renaud, A. *J. Chem. Soc., Faraday Trans. 1* **1981**, *77*, 1561.

(8) Gravereau, P.; Garnier, E.; Hardy, A. *Acta Crystallogr., Sect. B* **1979**, *35*, 2843.

10.1021/la063624c CCC: $37.00
Published on Web 04/03/2007

Table 1. Cell Edges, Degree of Hydration *x* (No. of Water Molecules per Formula Unit), Crystallite Size, and Estimated Density (in the Anhydrous State) for the Studied Materials

compound[a]	cell edges (Å)	*x*	crystallite size (Å)	density (g/cm^3)
Zn_3Co_2-C	$a = 10.2542(2$	11.8	734	1.28
Zn_3Co_2-R	$a = b = 12.4847(3)$ $c = 32.756(1)$	0.0	734[b]	1.41
Cd_3Co_2-C	$a = 10.591(1)$	13.6	366	1.45

[a] C − cubic (*Fm*-3*m*); R − rhombohedral (*R*-3*c*). [b] Zn_3Co_2-R was obtained from Zn_3Co_2-C.

thermal stability and degree of hydration were evaluated from the corresponding thermogravimetric (TG) curves. The materials' structural characterization was carried out from X-ray diffraction (XRD) data.

The TG curves were record using a TGA 2950 thermogravimetric analyzer (from TA Instruments) operated in high-resolution mode (Hi-ResTM). The heating rates were constrained to the range of 0.001 to 5 °C/min with an instrumental resolution of 5. The furnace was purged with nitrogen using a flow rate of 100 mL/min. IR spectra were collected using an FTIR spectrophotometer (Spectrum One from Perkin-Elmer) and the KBr pressed-disk technique. XRD powder patterns were recorded in Bragg−Brentano geometry by means of a D5000 diffractometer (from Siemens) and monochromatic Cu Kα radiation from 5 to 110° (2θ) using a step size of 0.025 and 25 s of counting time. XRD powder patterns under vacuum (10^{-5} Torr) were collected at the XPD beamline of the LNLS synchrotron radiation facility (at Campinas, Brazil) at a wavelength of 1.796760 Å from 5 to 110° (2θ) using a step size of 0.01. The crystallite size was estimated from the diffraction peak width.[9]

Xenon gas (Praxair, 99.999%) was used for both the Xe adsorption and ^{129}Xe NMR experiments. Before xenon adsorption, the samples were degassed under dynamic vacuum (10^{-4} Torr) for 4 h at 80 °C. In vacuum, the studied materials become anhydrous below 60 °C (discussed latter). The Xe adsorption isotherms were recorded using ASAP 2020 equipment (from Micromeritics). Sample tubes of a known weight were loaded with 100−200 mg of sample and sealed using a seal frit. Samples were degassed on the ASAP 2020 analyzer using a heating rate of 5 °C/min and then maintained at 80 °C for Cd_3Co_2-C and at 50 °C for Zn_3Co_2-R until a stable outgas rate below 10 μHg was obtained. The degassed sample and sample tube were weighed and then transferred back into the analyzer (with the seal frit preventing exposure of the sample to air). After the volume measurement with He, degassing was continued for 8 h at 80 °C in the sample port. Measurements were performed at 18 °C in a water bath at this temperature. The temperature was controlled using the Micromeritics Chiller Deward option and NESLAB refrigerated bath model RTE7 (temperature stability = ±0.01 °C). The obtained Xe adsorption isotherms were fitted according to the Langmuir−Freundlich equation

$$P = P_{0.5}\left(\frac{n_{ad}}{n_m - n_{ad}}\right)^g \quad (1)$$

derived from vacancy solution theory.[10] In eq 1, P is the absolute pressure, n_{ad} is the measured adsorption, n_m is the limit capacity of the micropores, $P_{0.5}$ is the pressure at $n_{ad} = 0.5n_m$, and g is the osmotic coefficient of the solution of vacancies and adsorbates and is related to the solution deviation from ideality.

To obtain ^{129}Xe NMR spectra, the sample powder was placed in an NMR tube equipped with J. Young valves, through which xenon gas was equilibrated at 18 °C for 30 min and under different pressures. ^{129}Xe NMR spectra were recorded at this temperature using a Bruker DMX-500 spectrometer operating at 138.34 MHz. Single excitation pulses were used with a recycle delay of 2 s, a 60° pulse width of 8 μs, and 1000−4000 scans. As a reference for the chemical shift values, an external sample of gaseous Xe was used, and the shift was then corrected to zero pressure using a reported procedure.[11]

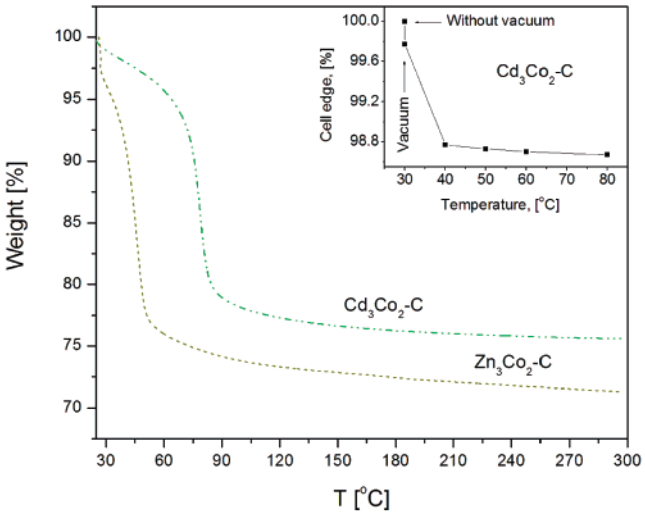

Figure 1. Thermogravimetric curves for the cadmium and zinc hexacyanocobaltates(III) (hydrated cubic phases). (Inset) Cell contraction on removal of the water of crystallization for cadmium hexacyanocobaltate(III). In vacuum, the dehydration process takes place at relatively low temperature.

3. Results and Discussion

A. On the Structure of the Studied Samples. The as-synthesized $Zn_3[Co(CN)_6]_2$ and $Cd_3[Co(CN)_6]_2 \cdot xH_2O$ samples were found to be rhombohedral (*R*-3*c*) and cubic (*Fm*-3*m*), respectively, in the following labeled as Zn_3Co_2-R and Cd_3Co_2-C. The corresponding XRD powder patterns, experimental and fitted, and the refined crystal structures are available as Supporting Information. Anhydrous cadmium hexacyanocobaltate(III) is hydrophilic and in the presence of water vapor saturates in only hours but preserves the *Fm*-3*m* structure. On aging in a humid atmosphere, the zinc compound (Zn_3Co_2-R) becomes hydrated through a structural transformation to a cubic (*Fm*-3*m*) phase (Zn_3Co_2-C). This structural change requires at least 1 week for completion. The zinc salt is dimorphic. The *R*-3*c* structure corresponds to its high-temperature modification, and compared with the cubic phase, it is a more compact structure (Table 1). Their calculated densities, as anhydrous phases, are 1.40 and 1.28 g/cm^3, respectively. Under atmospheric conditions, the stable phases of these two compounds correspond to the cubic (*Fm*-3*m*) unit cell typical of Prussian blue analogues.[5] In Table 1, the calculated cell edges for these three structures are reported.

The TG curves of the studied (cubic) samples as hydrates indicate that the water of crystallization is lost at relatively low temperature, about 80 °C, and then the resulting anhydrous phases remain stable above 250 °C (Figure 1). When heating is carried out in vacuum, the dehydration temperature decreases, and the compounds are found to be anhydrous below 60 °C (Figure 1, inset). According to the weight loss, the hydrated phases have 11.8 (Zn) and 13.6 (Cd) water molecules per formula unit; 6 of them are coordinated to the metal, which has a mixed coordination sphere, $M(NC)_4(H_2O)_2$. All of these water molecules fill the free space generated by the vacancy of the octahedral block, $[Co(CN)_6]$. The noncoordinated water molecules have zeolitic character and remain stabilized within the pores through hydrogen bonding interactions with the coordinated ones.

(9) Guinier, A. *X-ray Diffraction*; Dover Publications: Mineola, NY, 1994.
(10) Bering, B. P.; Serpinskii, V. V. *Izv. Akad. Nauk SSSR, Ser. Khim.* **1974**, *11*, 2427.
(11) Jameson, C. J.; Jameson, A. J.; Cohen, S. M. *J. Phys. Chem.* **1975**, *62*, 4424.

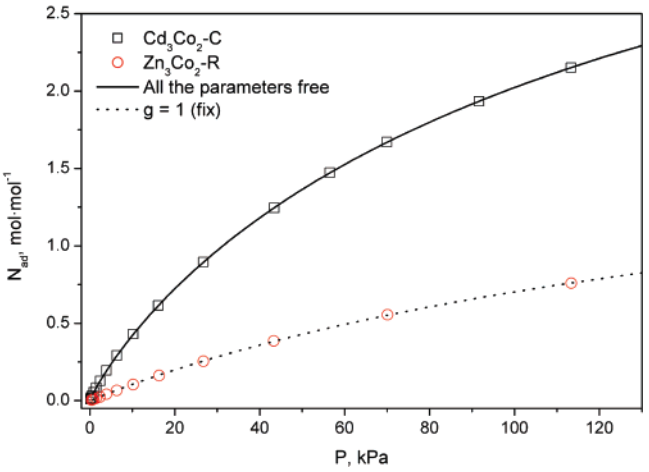

Figure 2. Xe adsorption curves at 18 °C in cadmium (cubic, *Fm*-3*m*) and zinc (*R*-3*c*) hexacyanocobaltate(III). The porous framework of the studied materials is accessible to Xe atoms. The stronger guest−host interaction is observed for Xe atom adsorption in the cubic structure.

The dehydration temperature of the zinc salt is particularly low. The polarizing power of Zn(2+) is higher than that of Cd(2+) (3.652 vs 2.041);[12] however, the latter has a stronger interaction with the coordinated water than the former. Such unusual behavior was attributed to the tendency of Zn(2+) to adopt a tetrahedral coordination with the N ends to form the anhydrous *R*-3*c* phase.

The loss of coordinated water molecules from the cadmium atom environment leads to certain cell contraction (Figure 1, inset). In the anhydrous form, the cadmium atom remains coordinated to only four CN groups. This enhances the metal (Cd) interaction with the ligands by subtracting charge from the CN group, particularly through its 5σ orbital, which has certain antibonding character. This induces a charge redistribution and an increase in π back-donation from the cobalt atom toward the CN group. The net effect is a stronger metal−metal interaction through the ligand and a shorter unit cell edge. The unit cell edge corresponds to the Cd−N≡C−Co−C≡N−Cd chain length.

B. Xe Adsorption Isotherms and Pore Accessibility to Xe Atoms. Xe has a kinetic diameter of 4.1 Å,[13] which is close to the pore window size (~4.5 Å). At low temperature, the porous framework of the studied materials was found to be practically inaccessible to the Xe atom. This agrees with previous adsorption studies in porous hexacyanometallates where the N_2 adsorption at −196 °C shows pronounced kinetic effects; as a consequence, to obtain an isotherm free of such effects, large equilibrium times are required.[6] Compared to Xe, the N_2 molecule has a smaller kinetic diameter, 3.86 Å.[13] Fortunately, when the probe species has sufficient kinetic energy its diffusion through narrow windows is facilitated. On the basis of this fact, the Xe adsorption in the studied materials was carried out at 18 °C, which is slightly above its critical temperature (T_c = 16.5 °C[13]), and the porous framework of both compounds was found to be accessible to the Xe atoms (Figure 2). Under such supercritical conditions, the Xe retention could be low but sufficient to explore the porous framework through ^{129}Xe NMR spectroscopy.

Figure 2 shows the Xe adsorption isotherms for the studied materials. These isotherms were fitted to eq 1. In Table 2, the obtained values for the involved parameters are reported. For Zn_3Co_2-R, the free variation of all of the parameters leads to g values close to 1, indicating that the Xe adsorption in this structure follows the Langmuir model. The Langmuir equation can be derived from statistical mechanics for a system of open and independent cavities that exchange energy and particles, assuming mobile adsorption without lateral interactions and with all of the molecules inside sensing the same adsorption energy.[14] Such considerations are appropriate for Xe adsorption in Zn_3Co_2-R. The pore surface of this structure is practically free of an electric field gradient. The ^{57}Fe Mössbauer spectrum of the iron analogue is an unresolved doublet with quadrupole splitting (Δ) of 0.236(3) mm/s.[15] That low value of Δ indicates that the iron nucleus is sensing a low electric field gradient in its environment. Such a low electric field gradient at the pore surface could be related to a relatively weak guest−host interaction for the Xe atoms within the pores, probably on the order of *kT*. On the basis of this fact, the adsorbed Xe atoms can be considered to be a mobile adsorbed phase. The unit cell for the rhombohedral phase contains six formula units of zinc cobalticyanide and three cavities (Supporting Information). The estimated limit capacity of micropores, which is close to 2 for $P \rightarrow \infty$, in units of mol/mol, is equivalent to 4 Xe atoms per cavity. Up to the maximum pressure allowed in our adsorption experiment, the effective pore filling remains below 1 Xe atom per cavity (Figure 2). This indicates relatively low pore volume occupation and probably weak lateral interactions between adsorbed Xe atoms, in correspondence with the Langmuir model hypothesis.

Table 2. Results Derived from the Xe Adsorption Isotherm Fitting According to Equation 1[a]

sample	N_m (mol·mol^{-1})	$P_{0.5}$ (kPa)	g	χ^2	R^2
Zn_3Co_2-R	1.92 ± 0.02	173 ± 2	1 (fix)	0.04633	0.99996
Cd_3Co_2-C	4.72 ± 0.03	138 ± 2	1.131 ± 0.004	0.00444	1

[a] R^2 is the coefficient of determination, and χ^2 is the chi-square value.

A qualitative evaluation of the isotherms shown in Figure 2 reveals that for the studied two typical structures, the stronger guest−host interactions and the higher porous framework ability of the Xe stabilization correspond to the cubic ones. The higher isotherm slope at low pressures is observed for Cd_3Co_2-C. When this isotherm was fitted according to eq 1, an osmotic coefficient (g) of 1.131(4) was obtained (Table 2). This value of g (>1) suggests a relatively strong vacancy−Xe interaction, in accordance with the qualitative consideration. The higher electric field gradient at the pore surface corresponds to the cubic structure, and this fact probably contributes to Xe adsorption through an induced quadrupole moment on the Xe atom. Xe is a large atom with an easily deformable electron cloud. Such a dispersive interaction could be facilitated by the smaller pore size in this structure. The cubic structure contains a cavity per formula unit with six metals of an unsaturated coordination sphere located at the cavity surface, which could be active sites for Xe adsorption. However, because of the relative large size of the Xe atom and the small cavity diameter (~8.5 Å), probably only a maximum of four Xe atoms could be accommodated within a cavity. The estimated limit capacity of micropores at $P \rightarrow \infty$, which resulted in 4.72(3) Xe atoms per formula unit (Table 2), exceeds the expected cavity capacity. This suggests that some Xe atoms could be adsorbed at interstitial positions (small pores) or in a mesoporous region related to the aggregation of small crystallites. At the maximum pressure allowed in our adsorption experiment,

(12) Zhang, Y. *Inorg. Chem.* **1982**, *21*, 3886.
(13) Medard, L., Ed. *Gas Encyclopaedia*, 3rd ed.; Elsevier: Amsterdam, 2002.
(14) Roque-Malherbe, R. *Physical Adsorption of Gases*; MES Ed.; Havana, 1987.
(15) Martinez-Garcia, R.; Knobel, M.; Reguera, E. *J. Phys. Chem. B* **2006**, *110*, 7296.

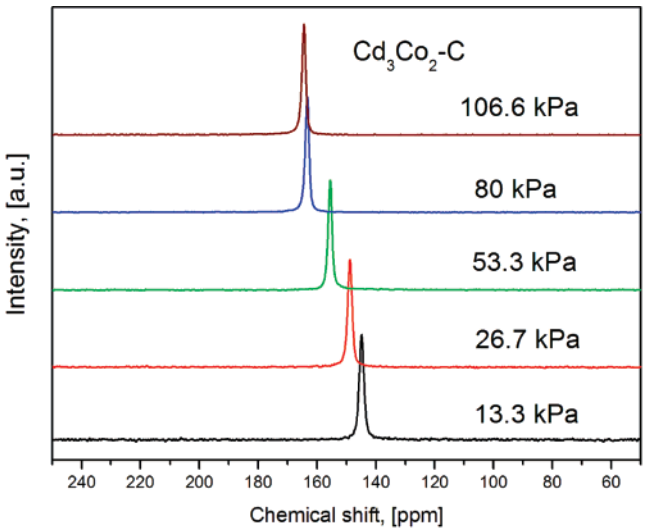

Figure 3. ^{129}Xe NMR spectra of Xe atoms adsorbed in the porous network of cadmium hexacyanocobaltate(III) (cubic phase).

more than 2 Xe atoms per formula unit are adsorbed. This value represents a relatively high pore-filling value for a supercritical gas. Under the mentioned relatively strong adsorption field for Xe in the cubic structure, this adsorbate probably undergoes a phase transition to a quasi-vapor state. Such a possibility is favored by the adsorption temperature that was used (18 °C), which is only slightly above the xenon critical temperature (16.1 °C).

No significant cell expansion related to the adsorption of Xe atoms is expected. The cell expansion and contraction in porous cyanometallates are closely related to the ability of the guest species to modify the electronic structure of the CN bridges through its interaction with the metals at the pore surface.[6] In the studied compounds, nonpolar guest species have a small capability to change the electronic structure of the host structure.[16] The Xe interaction with the metal at the pore surface must be weak, as is its effect on the interatomic distances.

C. ^{129}Xe NMR Spectra of Xe Atoms Adsorbed in Cadmium Cobalticyanide. Figure 3 shows ^{129}Xe NMR spectra of Xe atoms retained in the porous framework of anhydrous cadmium hexacyanocobaltate(III). These spectra are typical of an isotropic movement of Xe atoms (all of the tensor shielding components are equivalent), indicating that these atoms remain trapped within spherical cavities. For such a pore shape, certain empirical correlations between the ^{129}Xe chemical shift and the pore size are available.[17,18] The ^{129}Xe NMR chemical shift of adsorbed Xe atoms in porous solids has a different contribution[19]

$$\delta_{CS}(^{129}\mathrm{Xe}) = \delta_0 + \delta_S + \delta_{Xe} + \delta_{SAS} + \delta_E + \delta_M \quad (2)$$

where δ_0 is the chemical shift of gaseous Xe extrapolated to zero pressure, δ_S is the shift extrapolated to zero Xe loading, δ_{Xe} is the shift related to Xe−Xe interactions (collisions), δ_{SAS} is the contribution from strong adsorption sites, and δ_E and δ_M are contributions from electric and magnetic fields, respectively, at the adsorption sites. It has been suggested that the chemical shift of adsorbed xenon can be written as the sum of three terms corresponding to various perturbations at low xenon density:[17,19]

$$\delta_{CS}(^{129}\mathrm{Xe}) = \delta_0 + \delta_S + \delta_{Xe-Xe}\rho\mathrm{Xe} \quad (3)$$

In eq 3, the contribution from Xe−Xe collisions has been expressed in terms of the Xe atom concentration within the pore (ρ). The δ_S term arises from collisions between Xe atoms and the material pore surface, and it is estimated from an extrapolation of eq 3 to $\rho = 0$. In Figure 3, such a dependence is shown for Cd_3Co_2-C. The estimated value for δ_S is 143.6 ppm. The ^{129}Xe NMR spectra in the studied materials were recorded at a relatively low Xe load, at least compared with that of the above-discussed results from the adsorption experiments.

The value of δ_S depends on the mean free path $\langle L \rangle$ of a Xe atom within a pore. Usually, the larger the pore size, the smaller the value of δ_S. Such a dependence has been approximately expressed for zeolites through the following empirical expression:[18]

$$\delta_S = \frac{(243)(0.2054)}{0.2054 + \langle L \rangle} \quad (4)$$

The coefficient values depend on the chemical nature of the pore walls. According to the obtained value of δ_S in cadmium hexacyanocobaltate(III), within the pores of this material the value of $\langle L \rangle$ was estimated, using eq 4, to be 0.142 nm (1.42 Å). Because the pore generated by a $[M(CN)_6]$ vacancy may be approximated as a sphere (Figure 4, inset), this estimated $\langle L \rangle$ value corresponds to a pore diameter ($D_s = 2\langle L \rangle + 4.4$) of 7.2 Å. This is a reasonable result for the effective pore size that the Xe atom senses and is close to the estimated diameter of the free volume (ca. 8.41 Å) according to the unit cell edge of this material (10.59 Å) and the reported crystal radius for Cd(2+) in octahedral coordination (1.09 Å).[20] For the studied cadmium hexacyanocobaltate(III) sample, 13.6 water molecules per formula unit were found (Table 1). If within the pore the water of crystallization behaves as liquid water, with a molar volume of 18.06 mL/mol,[21] then the estimated pore volume will be 406 Å.^{3} For a spherical pore, this free space is equivalent to a pore diameter of 9.2 Å. This value probably represents a slight overestimation of the true pore size because within the pore the first six water molecules are located in the coordination environment of the Cd atom and the remaining ones are stabilized through relatively strong hydrogen bonding interactions with the coordinated ones and between them. In such a confined region, the water molecules could be more condensed than in the liquid state. In addition, the pore really is an octahedron, and the first six water molecules are located on its corners, a region that is probably inaccessible to the large Xe atom. From ^{129}Xe NMR spectra, a certain pore diameter underestimation is possibly related to repulsive interaction between the Xe atom and the CN electron cloud at the pore surface. For the water molecule, such an effect would be minimized.

D. ^{129}Xe NMR Spectra of Xe Atoms Adsorbed in Zinc Cobalticyanide. Figure 5 shows the ^{129}Xe NMR spectra of Xe atoms trapped within the porous framework of rhombohedral zinc hexacyanocobaltate(III). These spectra are typical of an anisotropic movement for the Xe atom indicating that it remains trapped within an elongated cavity where all of the components of the shielding tensor ($\sigma_{||}$, $\sigma_\perp$, and σ_t) are different. Xe NMR line shapes in nanochannels have been modeled and correlated with experimental results.[17,22,23] In the studied material, the cavity

(16) Martinez-Garcia, R.; Knobel, M.; Reguera, E. *J. Phys.: Condens. Matter* **2006**, *18*, 11243.
(17) Chen, F.; Chen, C. L.; Ding, S.; Yue, Y.; Ye, C.; Deng, F. *Chem. Phys. Lett.* **2004**, *383*, 309.
(18) Demarquay, J.; Fraissard, J. *Chem. Phys. Lett.* **1987**, *136*, 314.
(19) Ito, T.; Fraissard, J. *J. Chem. Phys.* **1982**, *76*, 5225.
(20) Shannon, R. D. *Acta Crystallogr., Sect. A* **1976**, *32*, 751.
(21) Lide, D.R., Ed. *CRC Handbook of Chemistry and Physics*, 77th ed.; Boca Raton, FL, 2006.
(22) Ripmestter, J. A.; Ratchiffe, I, C.; Tse, J. S. *J. Chem. Soc., Faraday Trans. 1* **1988**, *84*, 3731.

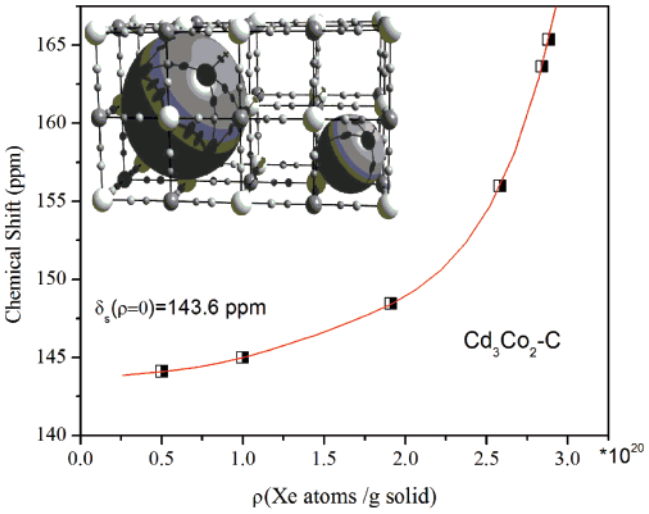

Figure 4. Dependence of the ^{129}Xe NMR chemical shift on the Xe density in Cd_3Co_2-C. Upon extrapolating the δ vs ρ dependence as $\rho \rightarrow 0$, the value of δ_s was estimated to be 143.6 ppm, which corresponds, according to eq 4, to a pore diameter of about 7.2 Å. (Inset) The larger sphere represents the pore created by a vacancy, and the smaller one, the interstitial free space that serves as pore windows.

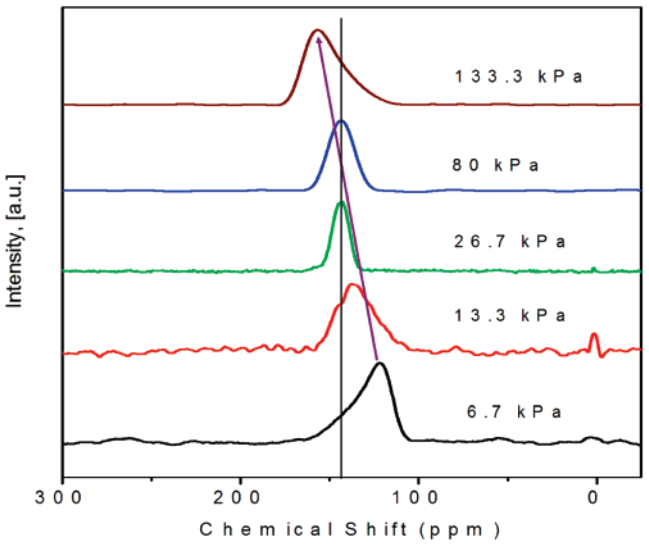

Figure 5. ^{129}Xe NMR spectra of Xe atoms adsorbed in the porous network of zinc hexacyanocobaltate(III) (rhombohedral phase). These spectra are characteristic of Xe atom movement within an elongated cavity.

could be approximated by an ellipsoidal pore. For such a pore shape, the Xe atom density becomes prolate where $\sigma_{||}$ includes the interaction with the entire wall arc of the cross-sectional plane. On the basis of this fact, σ_{II} must be the less shielded component, $\sigma_{||} < \sigma_{\perp} < \sigma$ (free Xe). Such ordering is valid for a single Xe atom within the cavity or in the absence of the Xe−Xe interaction of Xe atoms within neighboring cavities. When other Xe atoms could be present within the pore to form a dimer on the elliptical axis or Xe atoms within the neighboring cavities interact through the windows, the $\sigma_{\perp}$ component could be significantly changed. The Xe−Xe interactions will give rise to a large paramagnetic contribution to $\sigma_{\perp}$. In such case, this will be the less shielded component. This effect will be more pronounced as the Xe loading within the cavity increases, and the probability of Xe−Xe interaction through the windows of neighboring cavities is also larger.

The line shapes shown in Figure 5 can be explained in terms of the relative contributions of $\sigma_{||}$ and $\sigma_{\perp}$ components of the shielding tensor. At a Xe pressure of 6.7 kPa, the line shape is particularly asymmetric, indicating that the $\sigma_{||}$ and $\sigma_{\perp}$ components are quite different ($\sigma_{||} \ll \sigma_{\perp}$); however, at 26.6 kPa a narrow, symmetric line is obtained. At this Xe pressure, the effective shielding tensor is practically isotropic, $\sigma_{||} \approx \sigma_{\perp}$. Then, at 80 kPa the line broadens, and finally at 133.3 kPa it becomes asymmetric, $\sigma_{\perp} \ll \sigma_{||}$. This last pressure is equivalent to a Xe loading where the Xe−Xe interactions become the dominant contribution to the shielding.

Conclusions

^{129}Xe NMR spectra of Xe atoms adsorbed in cadmium and zinc hexacyanocobaltates(III) were recorded and studied. The porous frameworks of these compounds are accessible to the Xe atom. For cadmium, up to 2 Xe atoms per pore are adsorbed, which is ascribed to a relatively strong adsorption field for Xe with the pores of the *Fm*-3*m* structure and is probably related to the existence of an electric field gradient at the pore surface. A significantly weaker guest−host interaction was observed for the rhombohedral structure, where the pore surface has practically nonpolar character. For the cadmium complex salt, the ^{129}Xe NMR spectra are characteristic of the Xe atom movement within a spherical cavity. The estimated pore diameter from these spectra is in close agreement with the crystal structure of this material and also with the estimated pore volume from the calculated degree of hydration. The recorded ^{129}Xe NMR spectra of the rhombohedral phase of zinc hexacyanocobaltate(III) are characteristic of the Xe atom movement within an elongated cavity. The asymmetry of these spectra shows a marked dependence on the number of Xe atoms that have been charged within the porous framework. Such a dependence was ascribed to Xe−Xe interactions between Xe atoms located in neighboring cavities. The pore window size is large enough to allow these interactions.

Acknowledgment. This study was partially supported by CONACyT (Mexico) through cooperation project J200.813. The help of L. Reguera in the Xe adsorption data acquisition is acknowledged. We thank J. Rodríguez-Hernández for XRD data acquisition and processing. Access to the LNLS synchrotron radiation facility (at Campinas, Brazil) is also acknowledged.

Supporting Information Available: Experimental and fitted XRD powder patterns and their differences for the studied materials and crystal structure Rietveld refinement results (atomic positions, occupation and temperature factors, and estimated interatomic distances and bond angles). Metal coordination environment for the rhombohedral phase and the resulting pore geometry. Structural information has also been deposited at ICSD Fachinformationszentrum Karlsruhe (FIZ) (e-mail: crysdata@fiz-karlsruhe.de) with CSD file numbers 416744, $Zn_3[Co(CN)_6]_2 \cdot 12H_2O$ (cubic); 416740, $Zn_3[Co(CN)_6]_2$ (rhombohedral); and 416741, $Cd_3[Co(CN)_6]_2 \cdot 13H_2O$. This material is available free of charge via the Internet at http://pubs.acs.org.

LA063624C

(23) Jameson, C. J.; de Dios, A. C. *J. Chem. Phys.* **2002**, *116*, 3805.